PAPER *Special Section on Wideband Systems*

Performance Analysis of MIMO/FSO Systems Using SC-QAM Signaling over Atmospheric Turbulence Channels*

Trung HA DUYEN[†a)], ***Nonmember and*** **Anh T. PHAM**[††], ***Member***

SUMMARY We theoretically study the performance of multiple-input multiple-output (MIMO) free-space optical (FSO) systems using subcarrier quadrature modulation (SC-QAM) signaling. The system average symbol-error rate (ASER) is derived taking into account the atmospheric turbulence effects on the MIMO/FSO channel, which is modeled by log-normal and the gamma-gamma distributions for weak and moderate-to-strong turbulence conditions. We quantitatively discuss the influence of index of refraction structure parameter, link distance, and different MIMO configurations on the system ASER. We also analytically derive and discuss the MIMO/FSO average (ergodic) channel capacity (ACC), which is expressed in terms of average spectral efficiency (ASE), under the impact of various channel conditions. Monte Carlo simulations are also performed to validate the mathematical analysis, and a good agreement between numerical and simulation results is confirmed.

key words: *free-space optical (FSO) communications, multiple-input multiple-output (MIMO), subcarrier quadrature-amplitude modulation (SC-QAM), atmospheric turbulence, channel capacity*

1. Introduction

Free-space optical (FSO) communications, also known as optical-wireless communication, is a cost-effective, license-free, highly secured and broadband technique, which has recently received considerable attention for a variety of applications [1], [2]. One of major impairments to the performance of FSO systems is the influence of atmospheric turbulence, which is caused by variations in the refractive index due to inhomogeneties in temperature, pressure fluctuations, humidity changes, and motion of the air along the propagation path of the laser beam [3]. The atmospheric turbulence results in irradiance fluctuations in the received signal, i.e., the signal fading, which severely degrades the system performance, especially when the transmission distance is longer than 1 km [4].

Recent studies have shown that, similar to radio communications, the effect of fading over FSO links can be significantly relaxed by employing multiple-input multiple-output (MIMO) technique with multiple lasers at transmitter and multiple photodetectors at receiver. The first use of space diversity in FSO systems has been proposed in [5]. In [6] Lee and Chan have derived the outage probability of MIMO/FSO systems over log-normal turbulence channels. This study showed that the power gain of diversity increases as turbulence becomes stronger, and in theory, power gain of up to 25 dB could be achieved when the number of receivers approaches infinity. In [7], [8] Wilson et al. have formulated and analyzed symbol-error rate (SER) and bit-error rate (BER) of MIMO/FSO transmissions assuming pulse-position modulation (PPM) and Q-ary PPM in both log-normal and Rayleigh fading channels. In [9] Navidpour et al. have investigated the BER performance of MIMO/FSO links for both independent and correlated log-normal atmospheric turbulence channels. In [10], under the assumption of intensity-modulation/direct-detection (IM/DD) with on-off keying (OOK), a closed-form expression for the BER expression of single-input single-output (SISO) case and approximated closed-form BER expressions of MIMO/FSO links over strong turbulence channels in terms of Meijer's G-functions have been investigated.

Previous studies only focus on MIMO/FSO systems employing OOK and PPM modulation techniques. However, in the presence of atmospheric turbulence, OOK modulation needs an adaptive threshold to achieve its optimal performance [11]. On the other hand, PPM modulation has a poor bandwidth efficiency because of the fact that the narrow pulse is required for the high PPM multiplicities. To overcome the limitations of both OOK and PPM, subcarrier intensity modulation schemes, such as subcarrier phase-shift keying (SC-PSK) and quadrature-amplitude modulation (SC-QAM), have been considered for SISO/FSO systems. FSO system using SC-PSK signaling was first proposed by Huang et al. [11], and its performance over turbulence channels has been extensively investigated [12]–[15]. FSO system using SC-QAM has also gained attention due to its better spectral efficiency. In [16], Hassan et al. presented the average SER (ASER) for subcarrier intensity modulated wireless optical communications with general order rectangular QAM by using the series expansion of the modified Bessel function [17]. ASER of general-order rectangular QAM of FSO systems over atmospheric turbulence channels can be found in [18], [19]. Most recently, BER analysis of FSO systems with avalanche photodiode (APD) receiver over atmospheric turbulence channel have been reported [20]. However, to the best of our knowledge, the performance analysis of MIMO/FSO systems using SC-QAM signaling has not been reported in the literature.

In this paper, we therefore present a study on FSO systems employing both MIMO technique and SC-QAM sig-

Manuscript received March 15, 2013.
Manuscript revised July 27, 2013.
[†]The author is with School of Electronics and Telecommunications, Hanoi University of Science and Technology, Vietnam.
[††]The author is with the Computer Communications Lab., University of Aizu, Aizuwakamatsu-shi, 965-8580 Japan.
*The paper is presented in part at IEEE ICC 2013.
a) E-mail: trung.haduyen@hust.edu.vn
DOI: 10.1587/transfun.E97.A.49

naling in order to improve the system performance over atmospheric turbulence channels. We theoretically derive the ASER of considered systems, when both log-normal and gamma-gamma fading channels are assumed for weak and moderate-to-strong turbulence conditions, respectively. We also analytically derive and discuss the MIMO/FSO average (ergodic) channel capacity (ACC), which is expressed in terms of average spectral efficiency (ASE), under the impact of various channel conditions, system parameters and configurations. In addition, we validate the theoretical analysis by Monte Carlo simulations, a good agreement between numerical and simulation results is confirmed.

The remainder of the paper is organized as follows. In Sect. 2, the system descriptions and channel models are described. In Sect. 3, we present the performance analysis on the ASER of MIMO/FSO systems using SC-QAM signaling over log-normal and the gamma-gamma turbulence models. The analysis of system ACC is also included in this section. The numerical and Monte Carlo simulation results are provided in Sect. 4. Finally, we conclude the paper in Sect. 5.

2. System Descriptions

2.1 FSO System Using SC-QAM

The FSO system using SC-QAM signaling with single transmitter and single receiver (SISO system) is described in Fig. 1a. In this system, at the transmitter (Tx) side, each QAM symbol is first used to modulate an intermediate subcarrier frequency f_c by an electrical SC-QAM modulator; this up-converted electrical subcarrier QAM signal is then used to modulate the intensity of a laser. Generally, the electrical QAM signal can be given by

$$e(t) = s_I(t)\cos(2\pi f_c t) - s_Q(t)\sin(2\pi f_c t),\ 0 \leq t \leq T_s \quad (1)$$

where $s_I(t) = \sum_{i=-\infty}^{\infty} a_i(t) g(t - iT_s)$ is the in-phase signal and $s_Q(t) = \sum_{j=-\infty}^{\infty} b_j(t) g(t - jT_s)$ is the quadrature signal; $a_i(t)$ and $b_j(t)$ are the in-phase and the quadrature information signal amplitudes of the transmitted data symbol, respectively; $g(t)$ is the signal shaping pulse, and T_s is the symbol interval. Equivalently, the transmitted optical intensity can be given as

$$s(t) = P_s\{1 + \kappa[s_I(t)\cos(2\pi f_c t) - s_Q(t)\sin(2\pi f_c t)]\}, \quad (2)$$

where κ is the modulation index and $0 < \kappa \leq 1$. P_s denotes the average optical power per symbol. At the receiver (Rx) side, a telescope narrows the light beam and projects it toward the photodetector (PD). The received optical intensity, after being distorted over the turbulence channel, can be written as

$$r(t) = aXP_s\{1 + \kappa[s_I(t)\cos(2\pi f_c t) - s_Q(t)\sin(2\pi f_c t)]\}. \quad (3)$$

In this equation, a is the atmospheric attenuation factor, X represents the signal scintillation caused by atmospheric turbulence and can be modeled as a stationary random process. The DC term $\{aXP_s\}$ in Eq. (3) can be filtered out by a bandpass filter. The electrical signal at the photodetector (PD) output can be expressed as

$$r_e(t) = aXP_s\kappa\Re[s_I(t)\cos(2\pi f_c t) - s_Q(t)\sin(2\pi f_c t)] + \upsilon(t), \quad (4)$$

where $\Re$ denotes the PD's responsivity; $\upsilon(t)$ is receiver noise, which includes $\upsilon_I(t)$ and $\upsilon_Q(t)$, each can be modeled as additive white Gaussian noise (AWGN) process with power spectral density N_0. The electrical signal, $r_e(t)$, is then down-converted to the baseband to produce the in-phase signal $r_I(t)$ and the quadrature signal $r_Q(t)$ at the demodulator input as

$$r_I(t) = aXP_s\kappa\Re s_I(t) + \upsilon_I(t), \quad (5)$$

$$r_Q(t) = aXP_s\kappa\Re s_Q(t) + \upsilon_Q(t). \quad (6)$$

It is noted that carrier phase recovery is required for SC-QAM systems to obtain $r_I(t)$ and $r_Q(t)$. The received instantaneous electrical signal-to-noise ratio (SNR), γ, is a

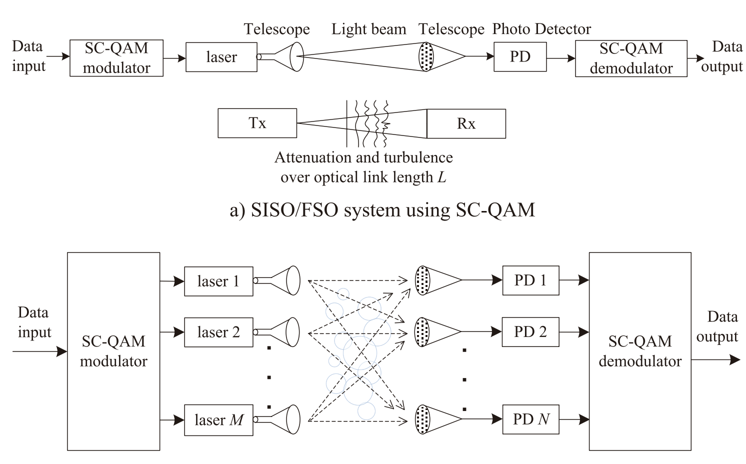

Fig. 1 Block diagram of SISO/FSO and $M{\times}N$ MIMO/FSO systems using SC-QAM signaling over atmospheric turbulence channel.

random variable (r.v.) given by $\gamma = (aXP_s\kappa\Re)^2/N_0$.

2.2 MIMO/FSO System Using SC-QAM

In this section, we consider a general $M{\times}N$ MIMO/FSO system using SC-QAM signaling with M lasers pointing toward an N-aperture receiver as depicted in Fig. 1(b). Data transmission with the same SC-QAM signal is transmitted with perfect synchronization by each of the M telescopes through an turbulence channel toward N PDs. The light beam-width of each telescope is assumed to be wide enough to illuminate the entire receiver array. The transmitter's telescope array is assumed to produce the same total optical power irrespective of M to enforce a fair comparison with the single transmitter case. The distance between the each transmitting telescope to the receiving one is assumed to be sufficient so that spatial correlation is negligible.

The MIMO/FSO channel can be modeled by an $M \times N$ matrix of the turbulence channel, denoted as $\mathbf{X} = [X_{mn}]_{m,n=1}^{M,N}$. Similar to Eq. (4), the electrical signal at the input of the QAM demodulator can be expressed as follows

$$r_e(t) = aP_s\Re\kappa e(t)\sum_{m=1}^{M}\sum_{n=1}^{N} X_{mn} + \upsilon(t), \quad n = 1, 2..., N, \quad (7)$$

where $e(t)$ represents the electrical QAM signal and $\upsilon(t)$ is the total receiver noise as defined above. X_{mn} denotes the stationary random process for the turbulence channel from the mth laser to the nth PD. When the equal gain combining (EGC) detector is employed at the receiver to estimate the transmitted signal, the instantaneous electrical SNR can be expressed as a finite sum of sub-channels as

$$\gamma = \left(\sum_{m=1}^{M}\sum_{n=1}^{N}\sqrt{\gamma_{mn}}\right)^2, \quad (8)$$

where γ_{mn} is the r.v. defined as the instantaneous electrical SNR component of the sub-channel from the mth laser to the nth PD, and it can be expressed as

$$\gamma_{mn} = \frac{(\frac{1}{MN}X_{mn}aP_s\Re\kappa)^2}{N_0} = \overline{\gamma}_{mn}X_{mn}^2, \quad (9)$$

in which, we denote $\overline{\gamma}_{mn}$ as the average electrical SNR contributed by the sub-channel between the mth laser and the nth PD. $\overline{\gamma}_{mn}$ is given by $\overline{\gamma}_{mn} = (\frac{1}{MN}aP_s\Re\kappa)^2/N_0$.

2.3 Atmospheric Turbulence Channel Models

When optical signal propagates through the FSO channel, the signal amplitude and phase are fluctuated due to the atmospheric turbulence. For weak turbulence conditions, the turbulence induced scintillation is assumed to be a random process that follows the log-normal distribution [18]; whereas for moderate-to-strong turbulence conditions, a gamma-gamma distribution is used [21].

2.3.1 Log-Normal Turbulence Model

In the log-normal turbulence channel, assuming that the average of scintillation is normalized to unity, the probability density function (pdf) for r.v. X_{mn} representing the turbulence of the sub-channel between the mth laser and the nth receiver can be described as [18]

$$f_{X_{mn}}(x) = \frac{1}{x\sigma_s\sqrt{2\pi}}\exp\left(-\frac{\left(\ln(x) + \frac{\sigma_s^2}{2}\right)^2}{2\sigma_s^2}\right), \quad (10)$$

where $\sigma_s^2 = \exp(\psi_1 + \psi_2) - 1$ with ψ_1 and ψ_1 being respectively given by

$$\psi_1 = \frac{0.49\sigma_2^2}{(1 + 0.18d^2 + 0.56\sigma_2^{12/5})^{7/6}}, \quad (11)$$

and

$$\psi_2 = \frac{0.51\sigma_2^2(1 + 0.69\sigma_2^{12/5})^{-5/6}}{1 + 0.9d^2 + 0.62d^2\sigma_2^{12/5}}. \quad (12)$$

In Eqs. (11) and (12), $d = \sqrt{kD^2/4L}$, where $k = 2\pi/\lambda$ is the optical wave number, L is the link distance in meters, λ is the optical wavelength, and D is the receiver aperture diameter of the PD. The parameter σ_2^2 is the Rytov variance and in this case, is expressed by [21]

$$\sigma_2^2 = 0.492C_n^2k^{7/6}L^{11/6}, \quad (13)$$

where C_n^2 is the index of refraction structure parameter, which is altitude-dependent and varies from 10^{-17} to $10^{-13}\mathrm{m}^{-2/3}$ accordingly to turbulence conditions.

2.3.2 Gamma-Gamma Turbulence Model

For the case of the gamma-gamma channel, the pdf of a normalized gamma-gamma r.v. X_{mn} is given as [21]

$$f_{X_{mn}}(x) = \frac{2(\alpha\beta)^{\frac{\alpha+\beta}{2}}}{\Gamma(\alpha)\Gamma(\beta)}x^{\frac{\alpha+\beta}{2}-1}K_{\alpha-\beta}\left(2\sqrt{\alpha\beta x}\right), \quad (14)$$

where $\Gamma(\cdot)$ is the Gamma function and $K_{\alpha-\beta}(\cdot)$ is the modified Bessel function of the second kind of order $(\alpha - \beta)$, while the parameters α and β are directly related to atmospheric conditions through the following expression:

$$\alpha = \left[\exp(\psi_1) - 1\right]^{-1}, \quad \beta = \left[\exp(\psi_2) - 1\right]^{-1}. \quad (15)$$

The parameters α and β are related with the scintillation index by

$$SI = \frac{1}{\alpha} + \frac{1}{\beta} + \frac{1}{\alpha\beta}. \quad (16)$$

Figure 2 shows the pdf for a few instances of the turbulence strength. For $SI < 0.8$, the gamma-gamma distribution resembles a log-normal distribution. The gamma-gamma distributions with turbulence strength values of $SI =$

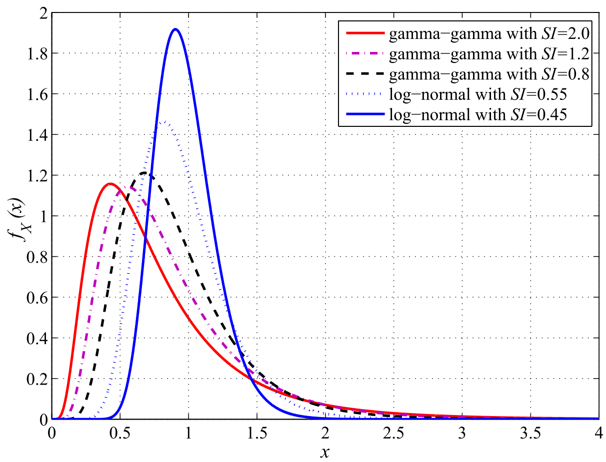

Fig. 2 pdfs of different log-normal and gamma-gamma intensity distributions.

0.8, $SI = 1.2$, and $SI = 2.0$ are quite different with smaller amplitudes than the log-normal distributions in two specific cases of $SI = 0.45$ and $SI = 0.55$. In particular, the gamma-gamma model has higher density in the low amplitude region, resulting in a more unexpected impact on the system performance.

3. Performance Analysis

3.1 ASER Derivation

The atmospheric turbulence channel can be modeled as a slow-fading process because its temporal correlation time, which is on the order of several milliseconds, is much larger than the QAM symbol duration. The ASER averaged over the turbulence channel therefore can be expressed as

$$\overline{P}_{se}^{MIMO} = \int_{\mathbf{\Gamma}} P_e(\gamma) \times f_{\mathbf{\Gamma}}(\Gamma) d\Gamma. \tag{17}$$

Here, γ is the instantaneous electrical SNR, which is a function of γ_{mn} as given in Eq. (8). $\mathbf{\Gamma} = \{\Gamma_{nm}, n = 1, ..., N, m = 1, ..., M\}$ is the matrix of the MIMO atmospheric turbulence channels. $P_e(\gamma)$ is the conditional error probability (CEP) of the received instantaneous electrical SNR. For SC-QAM systems, the CEP $P_e(\gamma)$ is given by [22]

$$P_e(\gamma) = 1 - [1 - 2q(M_I)Q(A_I\sqrt{\gamma})][1 - 2q(M_Q)Q(A_Q\sqrt{\gamma})], \tag{18}$$

where M_I and M_Q are respectively in-phase and quadrature signal amplitudes, $q(x) \triangleq 1 - x^{-1}$, $Q(x) \triangleq 1/\sqrt{2\pi}\int_x^\infty \exp(-t^2/2)dt$ is the Gaussian Q-function which relates to the terms of the complementary error function erfc(·) by $Q(x) = \frac{1}{2}\text{erfc}(x/\sqrt{2})$, $A_I = (6/[(M_I^2 - 1) + r^2(M_Q^2 - 1)])^{1/2}$, and $A_Q = (6r^2/[(M_I^2 - 1) + r^2(M_Q^2 - 1)])^{1/2}$, in which $r = d_Q/d_I$ is the quadrature to in-phase decision distance ratio.

Equation (18) can further be written as follows

$$\begin{aligned} P_e(\gamma) = &\, 2q(M_I)Q(A_I\sqrt{\gamma}) + 2q(M_Q)Q(A_Q\sqrt{\gamma}) \\ &- 4q(M_I)q(M_Q)Q(A_I\sqrt{\gamma})\,Q(A_Q\sqrt{\gamma}). \end{aligned} \tag{19}$$

By replacing (19) into (17), ASER of the MIMO systems can be derived as

$$\begin{aligned} \overline{P}_{se}^{MIMO} = &\, 2q(M_I)\int_{\mathbf{\Gamma}} Q(A_I\sqrt{\gamma})\, f_{\mathbf{\Gamma}}(\Gamma)d\Gamma \\ &+ 2q(M_Q)\int_{\mathbf{\Gamma}} Q(A_Q\sqrt{\gamma})\, f_{\mathbf{\Gamma}}(\Gamma)d\Gamma \\ &- 4q(M_I)q(M_Q)\int_{\mathbf{\Gamma}} Q(A_I\sqrt{\gamma})Q(A_Q\sqrt{\gamma})\, f_{\mathbf{\Gamma}}(\Gamma)d\Gamma. \end{aligned} \tag{20}$$

Assuming that MIMO sub-channels' turbulence processes are uncorrelated, independent and identically distributed (i.i.d.), the joint pdf $f_{\mathbf{\Gamma}}(\Gamma)$ can be reduced to a product of the first-order pdf of each element Γ_{mn} [23]. From Eqs. (9), (10) and (14), the pdf of the r.v. Γ_{mn} in case of weak and moderate-to-strong turbulence channels can be, respectively, given as

$$f_{\Gamma_{mn}}(\gamma_{mn}) = \frac{1}{2\gamma_{mn}\sigma_s\sqrt{2\pi}} \exp\left(-\frac{\left(\ln\left(\frac{\gamma_{mn}}{\overline{\gamma}_{mn}}\right) + \sigma_s^2\right)^2}{8\sigma_s^2}\right), \tag{21}$$

and,

$$f_{\Gamma_{mn}}(\gamma_{mn}) = \frac{(\alpha\beta)^{\frac{\alpha+\beta}{2}}}{\Gamma(\alpha)\Gamma(\beta)} \frac{\gamma_{mn}^{\frac{\alpha+\beta}{4}-1}}{\overline{\gamma}_{mn}^{\frac{\alpha+\beta}{4}}} K_{\alpha-\beta}\left(2\sqrt{\alpha\beta\sqrt{\frac{\gamma_{mn}}{\overline{\gamma}_{mn}}}}\right). \tag{22}$$

3.2 Average Channel Capacity

In this section, we analytically derive the average channel capacity (ACC) for the $M\times N$ MIMO/FSO link in the presence of atmospheric turbulences. This is a crucial metric for evaluating the optical link performance. The ACC can also be expressed in terms of average spectral efficiency (ASE) in bits/s/Hz if the frequency response of the channel is known. We assume that the optical channel is memoryless, stationary, ergodic with i.i.d. turbulence statistics and perfect channel state information (CSI) is available at both the transmitting lasers and the aperture receivers, the system ASE can be defined as

$$\frac{\overline{C}}{B} = \int_{\mathbf{\Gamma}} \log_2(1+\gamma) f_{\mathbf{\Gamma}}(\Gamma)d\Gamma, \quad \text{(bit/s)} \tag{23}$$

where B is the channel's bandwidth and γ is the total channel SNR as given in Eq. (8) and $\mathbf{\Gamma} = \{\Gamma_{nm}, n = 1, ..., N, m = 1, ..., M\}$ is the matrix of the MIMO atmospheric turbulence channels. Similarly, the joint pdf $f_{\mathbf{\Gamma}}(\Gamma)$ can be reduced to a product of the first-order pdf of each element Γ_{mn}. The pdf of the r.v. Γ_{mn} in case of log-normal and gamma-gamma channels are given in Eqs. (21) and (22), respectively. As a result, the system ASE expressed in Eq. (23) can be calculated through multi-dimensional numerical integration.

3.2.1 Capacity of Log-Normal MIMO/FSO Channels

Using (21) and (23), the ASE of a log-normal MIMO/FSO

$$\frac{\overline{C}}{B} = C_0\left(\sum_{k=1}^{\infty}\frac{(-1)^{k+1}}{k}\left[\mathrm{erfcx}\left(\sqrt{2}\sigma_s k+\frac{\Gamma_{mn}}{2\sqrt{2}\sigma_s}\right)+\mathrm{erfcx}\left(\sqrt{2}\sigma_s k-\frac{\Gamma_{mn}}{2\sqrt{2}\sigma_s}\right)\right]+\frac{4\sigma_s}{\sqrt{2\pi}}+\Gamma_{mn}\exp\left(\frac{\Gamma_{mn}^2}{8\sigma_s^2}\right)\mathrm{erfc}\left(-\frac{\Gamma_{mn}}{2\sqrt{2}\sigma_s}\right)\right), \tag{25}$$

channel can be expressed as

$$\frac{\overline{C}}{B} = \frac{1}{2\sigma_s\sqrt{2\pi}\ln(2)}\int_{\Gamma}\frac{\ln(1+\gamma_{mn})}{\gamma_{mn}} \times \exp\left(-\frac{\left(\ln\left(\frac{\gamma_{mn}}{\overline{\gamma}_{mn}}\right)+\sigma_s^2\right)^2}{8\sigma_s^2}\right)d\gamma_{mn}. \tag{24}$$

Using the equality $\ln(1+x)=\sum_{k=1}^{+\infty}(-1)^{k+1}x^k/k$, $(0\leq x\leq 1)$, and the scaled complementary error function $\mathrm{erfcx}(x)= e^{x^2}\mathrm{erfc}(x)$, the integral (24) can be transformed to the summation in Eq. (25). In Eq. (25), $\Gamma_{mn}=\ln(\overline{\gamma}_{mn})-\sigma_s^2$ with $\overline{\gamma}_{mn}$ is the instantaneous received SNR output of EGC detector, and $C_0=\exp(-\Gamma^2/8\sigma_s^2)/2\ln 2$.

3.2.2 Capacity of Gamma-Gamma MIMO/FSO Channels

Substituting (22) into (23), the average capacity of a gamma-gamma MIMO/FSO channel can be given by

$$\frac{\overline{C}}{B} = \frac{\left(\frac{\alpha\beta}{\sqrt{\overline{\gamma}_{mn}}}\right)^{\frac{\alpha+\beta}{2}}}{\Gamma(\alpha)\Gamma(\beta\ln(2)}\int_{\Gamma}\ln(1+\gamma_{mn}) \times \gamma_{mn}^{\frac{\alpha+\beta}{4}-1}K_{\alpha-\beta}\left(2\sqrt{\alpha\beta\sqrt{\frac{\gamma_{mn}}{\overline{\gamma}_{mn}}}}\right)d\gamma_{mn}. \tag{26}$$

Using the Meijer G-function, $\mathrm{G}_{mn}^{pq}[\cdot]$, to express the logarithmic term of $\ln(1+x)=\mathrm{G}_{2,2}^{1,2}\left[x\middle|_{1,0}^{1,1}\right]$ ([24], Eq. (11)), and $K_{\vartheta}(x)=\frac{1}{2}\mathrm{G}_{0,2}^{2,0}\left[\frac{x^2}{4}\middle|_{\frac{\vartheta}{2},-\frac{\vartheta}{2}}^{-,\ -}\right]$ ([24], Eq. (14)), the ASE can be expressed by

$$\frac{\overline{C}}{B}=\frac{\left(\frac{\alpha\beta}{\sqrt{\overline{\gamma}_{mn}}}\right)^{c/2}}{4\pi\Gamma(\alpha)\Gamma(\beta)\ln(2)}\mathrm{G}_{2,6}^{6,1}\left[\frac{(\alpha\beta)^2}{16\overline{\gamma}_{mn}}\middle|_{\frac{d}{4},\frac{d+2}{4},-\frac{d}{4},-\frac{c}{4},-\frac{c}{4}}^{-\frac{c}{4},-\frac{c}{4}+1}\right], \tag{27}$$

where $c=\alpha+\beta$ and $d=\alpha-\beta$.

4. Numerical Results and Discussions

In this section, we evaluate the ASER for different values of C_n^2: 1×10^{-15} $\mathrm{m}^{-2/3}$, 9×10^{-15} $\mathrm{m}^{-2/3}$, and 3×10^{-14} $\mathrm{m}^{-2/3}$ for weak, moderate, and strong turbulence conditions, respectively. The log-normal distribution model is used for weak turbulence condition; whereas the gamma-gamma distribution model is used for moderate-to-strong turbulence conditions. We use the receiver aperture with diameter $D=0.08$ m, and the operational wavelength $\lambda=1.55$ μm, while for the free-space link, different values of distance L from 1,000 m to 6,000 m are selected. In addition, unless otherwise noted, the 8×4 SC-QAM is assumed.

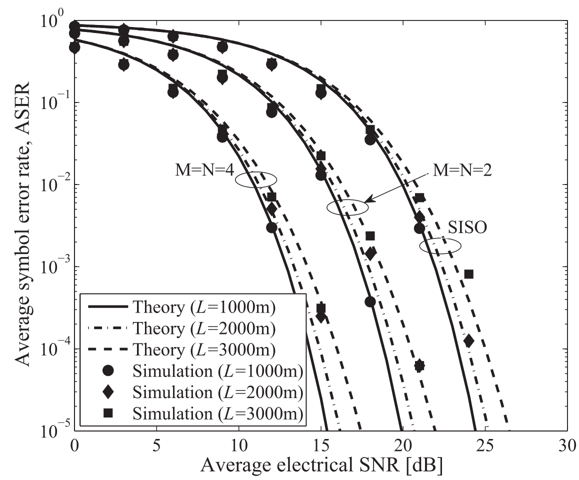

Fig. 3 ASER versus average SNR, $\overline{\gamma}$, of SISO/FSO system, 2×2 and 4×4 MIMO/FSO systems using 8×4 SC-QAM for various values of L with $C_n^2=1\times10^{-15}$ $\mathrm{m}^{-2/3}$.

Figure 3 illustrates the ASER as a function of the average electrical SNR, $\overline{\gamma}=(\frac{1}{MN}a\Re P_s\kappa)^2/N_0$, for different values of link distance L. We consider different MIMO configurations of 2×2 and 4×4 for FSO systems using SC-QAM over weak atmospheric turbulence with $C_n^2=1\times10^{-15}$ $\mathrm{m}^{-2/3}$. The performance of SISO/FSO system (i.e. when $M=N=1$) is also included as a benchmark. As it is clearly shown, the performance is improved significantly with the increase of number of lasers and receivers, which, as a result, could reduce the required SNR for a certain ASER. More specifically, power gains when the MIMO configuration changes from SISO to 2×2 MIMO or 2×2 MIMO to 4×4 MIMO are about 5 dB at the ASER of 10^{-5}. The numerical results, calculated with the help of Eqs. (20) and (21), are also compared with the corresponding Monte Carlo simulations, which are presented with dark markers in circles, diamonds, and squares. It can be observed that the theoretical results closely agree with the simulations.

In Figs. 4, 5, the impacts of C_n^2 on the error performance of various system configurations with link distances $L=2,000$ and $4,000$ m are analyzed. In all cases of the numerical results, Monte Carlo simulations are also performed. As can be observed, the system performance is strongly depends on C_n^2, especially in case of longer link distances. This is because the turbulence strength will become strong as the link distance increases. For instance, by comparing the two figures, it is seen that for the 4×4 MIMO/FSO system with the weak turbulence with $C_n^2=1\times10^{-15}$, the average electrical SNRs required to achieve the ASER of 10^{-5} for $L=2,000$ and $4,000$ are 17 and 20.5 dB, respectively.

In Fig. 6, we shows the ASER performance of SISO

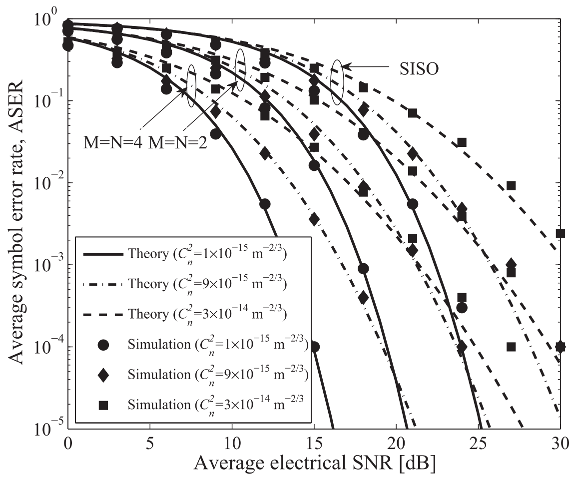

Fig. 4 ASER versus the average SNR, $\overline{\gamma}$, of SISO/FSO system, 2×2 and 4×4 MIMO/FSO systems using 8×4 SC-QAM for various values of C_n for weak, moderate, and strong atmospheric turbulence conditions with free-space link distance of $L = 2,000$ m.

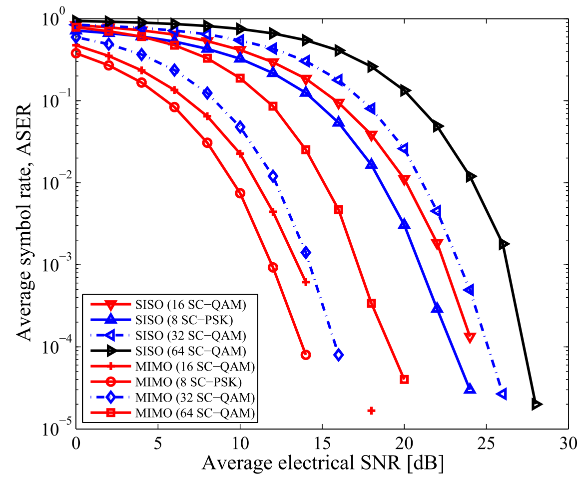

Fig. 6 ASER versus the average SNR, $\overline{\gamma}$, of SISO/FSO and 4×4 MIMO/FSO systems with different QAM multiplicities; $C_n^2 = 1 \times 10^{-15} \mathrm{m}^{-2/3}$, and free-space link distance $L = 2,000$ m.

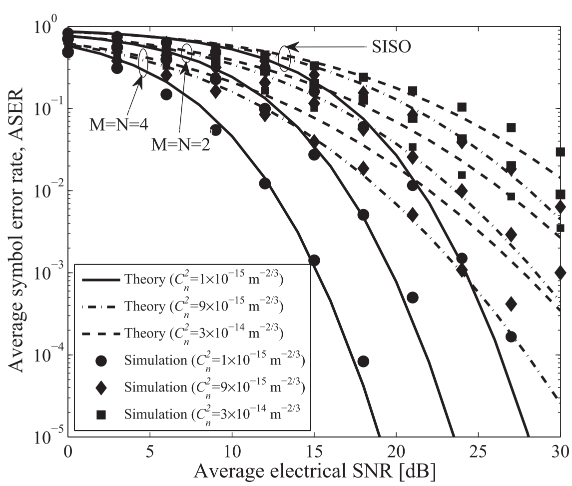

Fig. 5 ASER versus the average SNR, $\overline{\gamma}$, of SISO/FSO system, 2×2 and 4×4 MIMO/FSO systems using 8×4 SC-QAM for various values of C_n for weak, moderate, and strong atmospheric turbulence conditions with free-space link distance $L = 4,000$ m.

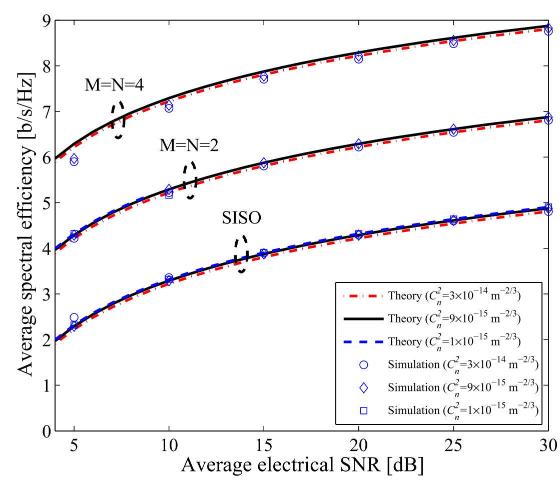

Fig. 7 ASE, $\overline{C}/B$, versus the average electrical SNR, $\overline{\gamma}$, of different MIMO/FSO channels for different values of C_n^2 with free-space link distance $L = 1,000$ m.

and MIMO/FSO systems vs. the average electrical SNR for different SC-QAM multiplicities, from 8 to 64. The link distance $L = 2,000$ m and $C_n^2 = 1 \times 10^{-15}$. It is also seen that MIMO significantly improve the FSO system with different SC-QAM multiplicities under the impact of atmospheric turbulence. The power gain of approximately 9 dB is seen when the target ASER is less than 10^{-3}.

Next, using derived expressions of (25) and (27), we evaluate the ASE of MIMO/FSO channels as a function of the average electrical SNR at the receiver, $\overline{\gamma}$. We use (25) for weak turbulence with log-normal channel model, while (27) is used for moderate-to-strong turbulences with the gamma-gamma channel model. We use the system parameters and different values of C_n^2 and link distance L, as discussed above. SISO/FSO channel is also included in the numerical results as a benchmark. And again, the Monte Carlo simulation is used to validate the theoretical analysis as the expressions derived in (25) and (27). As it is seen, the well-matched results confirm the validity of the theoretical analysis.

Figures 7–9 illustrate the ASE of different MIMO/FSO channels (i.e., 2×2 and 4×4 MIMO/FSO channels) with respect to $\overline{\gamma}$, for different values of C_n^2 and link distances. It can be also seen that the ASE strongly depends on C_n^2, especially when the link distance gets longer. For instance, when $L = 1,000$ m, the ASEs for different C_n^2 are also the same while for the case $L = 6,000$ m, the ASE at SNR = 15 dB for SISO/FSO link decreases from 4 to 3 b/s/Hz when C_n^2 increases from 1×10^{-15} to 3×10^{-14}. This is a logical result as the influence of atmospheric turbulence becomes stronger as the link distance increases. On the other hand, as expected, the ASE could be improved by approximately 2 (b/s/Hz) when the system is upgraded from SISO/FSO

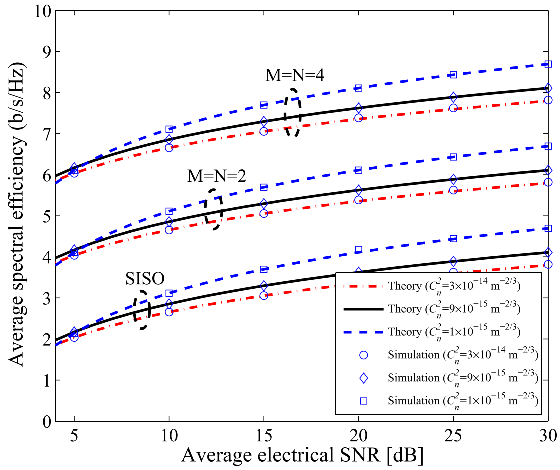

Fig. 8 ASE, $\overline{C}/B$, versus the average electrical SNR, $\overline{\gamma}$, of different MIMO/FSO channels for different values of C_n^2 with free-space link distance $L = 3,000$ m.

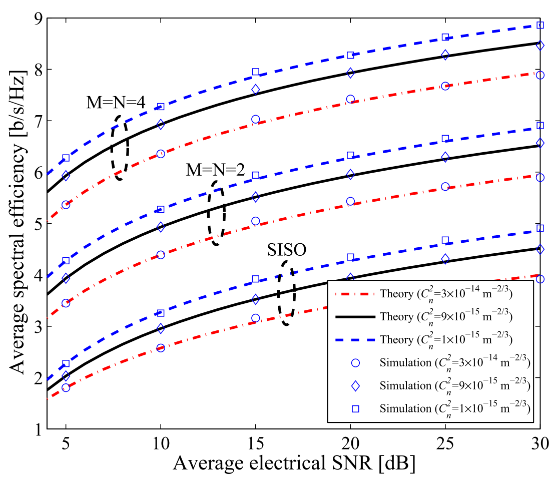

Fig. 9 ASE, $\overline{C}/B$, versus the average electrical SNR, $\overline{\gamma}$, of different MIMO/FSO channels for different values of C_n^2 with free-space link distance $L = 6,000$ m.

to 2×2 MIMO/FSO or from 2×2 MIMO/FSO to 4×4 MIMO/FSO.

5. Conclusions

We have presented the performance analysis on the average channel capacity and ASER of MIMO/FSO systems using SC-QAM signaling over atmospheric turbulence channels. The log-normal and gamma-gamma distributions were used to model the fluctuation of the optical propagating over atmospheric turbulence channels. We analytically derived the system ASER and ASE considering different link conditions and MIMO configurations. Monte Carlo simulations were also performed to validate the theoretical analysis, and a good agreement between theoretical and simulation results has been confirmed. It was seen that, with the similar link distance and C_n^2, when the FSO system is upgraded from SISO to 2×2 MIMO or 2×2 MIMO to 4×4 MIMO, an average gain of approximately 5 dB at the ASER of 10^{-5} could be obtained. As well, regardless the link distance and turbulence condition, the ASE of the FSO link could be improved by approximately 2 (b/s/Hz) when the system is upgraded from SISO/FSO to 2×2 MIMO/FSO or from 2×2 MIMO/FSO to 4×4 MIMO/FSO.

Acknowledgments

The first author is funded by the Vietnam National Foundation for Science and Technology Development (NAFOSTED) under grant number 102.02-2011.15 and the Visiting Researcher program of the University of Aizu, Japan.

References

[1] H. Willebrand and B.S. Ghuman, Free Space Optics: Enabling Optical Connectivity in Today's Networks, Indianapolis, Sams Publishing, IN, 2002.

[2] D. Kedar and S. Arnon, "Urban optical wireless communication networks: The main challenges and possible solutions," IEEE Commun. Mag., vol.42, no.5, pp.2–7, May 2004.

[3] X. Zhu and J.M. Kahn, "Free-space optical communication through atmospheric turbulence channels," IEEE Trans. Commun., vol.50, no.8, pp.1293–1300, Aug. 2002.

[4] L. Andrews, R.L. Philips, and C.Y. Hopen, Laser Beam Scintillation With Applications, SPIE Press, 2001.

[5] M.M. Ibrahim and A.M. Ibrahim, "Performance analysis of optical receivers with space diversity reception," Proc. IEE-Commun., vol.143, no.6, pp.369–372, Dec. 1996.

[6] E. Lee and V. Chan, "Part 1: Optical communication over the clear turbulence atmospheric channel using diversity," IEEE Trans. Commun., vol.22, no.9, pp.1896–1960, Nov. 2004.

[7] S.G. Wilson, M. Brandt-Pearce, Q. Cao, and J.H. Leveque, "Free-space optical MIMO transmission with Q-ary PPM," IEEE Trans. Commun., vol.53, no.8, pp.1402–1412, Aug. 2005.

[8] S.G. Wilson, M. Brandt-Pearce, Q. Cao, and J.H. Leveque, "Optical repetition MIMO transmission with multiple PPM," IEEE J. Sel. Areas Commun., vol.23, no.9, pp.1901–1910, Sept. 2005.

[9] S.M. Navidpour, M. Uysal, and M. Kavehrad, "BER performance of free-space optical transmission with diversity," IEEE Trans. Wireless Commun., vol.6, no.8, pp.1402–1412, Aug. 2007.

[10] T.A. Tsiftsis, H.G. Sandalidis, G.K. Karagiannidis, and M. Uysal, "FSO links with spatial diversity over strong atmospheric turbulence channels," Proc. ICC'08, pp.5379–5384, May 2008

[11] W. Huang, J. Takayanagi, T. Sakanaka, and M. Nakagawa, "Atmospheric optical communication system using subcarrier PSK modulation," IEICE Trans. Commun., vol.E76-B, no.9, pp.1169–1177, Sept. 1993.

[12] J. Li, J.Q. Liu, and D.P. Taylor, "Optical communication using subcarrier PSK intensity modulation through atmospheric turbulence channels," IEEE Trans. Commun., vol.55, pp.1598–1606, Aug. 2007.

[13] W.O. Popoola and Z. Ghassemlooy, "BPSK subcarrier intensity modulated free-space optical communications in atmospheric turbulence," J. Lightwave Technol., vol.27, pp.967–973, April 2009.

[14] A. Pham, T. Thang, S. Guo, and Z. Cheng, "Performance bounds for turbo-coded sc-psk/fso communications over strong turbulence channels," Proc. IEEE Int. Conf. on Advanced Tech. for Commun. (ATC'11), pp.161–164, Aug. 2011.

[15] X. Song, M. Niu, and J. Cheng, "Error rate of subcarrier intensity modulations for wireless optical communications," IEEE Commun. Lett., vol.16, pp.540–543, April 2012.

[16] Md. Z. Hassan, X. Song, and J. Cheng, "Subcarrier intensity modulated wireless optical communications with rectangular QAM," J.

Opt. Commun. Netw., vol.4, no.6, pp.522–532, June 2012.
[17] E. Bayaki, R. Schober, and R.K. Mallik, "Performance of MIMO free-space optical systems in gamma-gamma fading," IEEE Trans. Commun., vol.57, no.11, pp.3415–3424, Nov. 2009.
[18] K.P. Peppas and C.K. Datsikas, "Average symbol error probability of general-order rectangular quadrature amplitude modulation of optical wireless communication systems over atmospheric turbulence channels," J. Opt. Commun. Netw., vol.1, no.2, pp.102–110, Feb. 2010.
[19] M.Z. Hassan, X. Song, and J. Cheng, "Subcarrier intensity modulated wireless optical communications with rectangular QAM," J. Opt. Commun. Netw., vol.4, no.6, pp.522–532, June 2012.
[20] B.T. Vu, C.T. Truong, A.T. Pham, and N.T. Dang, "Bit-error rate analysis of rectangular QAM/FSO systems using APD receiver over atmospheric turbulence channels," IEEE/OSA J. Opt. Commun. and Netw., vol.5, no.5, pp.437–446, May 2013.
[21] A.K. Majumdar, "Free-space laser communication performance in the atmospheric channel," J. Opt. Fiber Commun. Rep., vol.2, no.4, pp.345–396, 2005.
[22] A. Maaref and S. Aissa, "Exact error probability analysis of rectangular QAM for single- and multichannel reception in Nakagami-m fading channels," IEEE Trans. Commun., vol.57, no.1, pp.214–221, Jan. 2009.
[23] N. Cvijetic, S.G. Wilson, and M. Brandt-Pearce, "Performance bounds for free-space optical MIMO systems with APD receivers in atmospheric turbulence," IEEE J. Sel. Areas Commun., vol.26, no.3, pp.3–12, April 2008.
[24] V.S. Adamchik and O.I. Marichev, "The algorithm for calculating integrals of hypergeometric type functions and its realization in reduce system," Int. Conf. on Symbolic and Algebraic Computation, pp.212–224, Tokyo, Japan, 1990.

Trung Ha Duyen received the B.Eng. degree in Electronics and Telecommunications from Hanoi University of Technology, Vietnam, and the MSc and PhD degrees in Communications Engineering from Chulalongkorn University, Thailand in 2005 and 2009, respectively. Since September 2009, he has been lecturer and assistant professor at the School of Electronics and Telecommunications, Hanoi University of Science and Technology. From 2007 to 2008, he was a visiting research student at the Tokyo Institute of Technology, Japan. In 2012, Dr. Trung spent 3 months as a visiting researcher at the University of Aizu, Japan. His present research interests are in the area of Free-Space Optical and MIMO communications, GNSS and its applications. Dr. Trung received Japanese International Cooperation Agency (JICA) scholarship for his MSc and PhD studies.

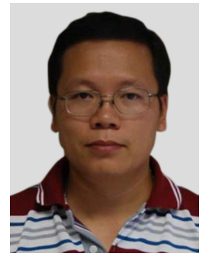

Anh T. Pham received the B.E. and M.E. degrees, both in Electronics Engineering from the Hanoi University of Technology, Vietnam in 1997 and 2000, respectively, and the Ph.D. degree in Information and Mathematical Sciences from Saitama University, Japan in 2005. From 1998 to 2002, he was with the NTT Corp. in Vietnam. Since April 2005, he has been on the faculty at the University of Aizu, where he is currently a senior associate professor at the Computer Communications Laboratory, the School of Computer Science and Engineering. Dr. Pham's research interests are in the broad areas of communication theory and networking with a particular emphasis on modeling, design and performance evaluation of wired/wireless communication systems and networks. He received Japanese government scholarship (MonbuKagaku-sho) for Ph.D. study. He also received Vietnamese government scholarship for undergraduate study. Dr. Pham is senior member of IEEE. He is also member of IEICE and OSA.